JACS Au
AN OPEN ACCESS JOURNAL OF THE AMERICAN CHEMICAL SOCIETY

pubs.acs.org/jacsau

Article

# Broadly Neutralizing Synthetic Cannabinoid Vaccines

Mingliang Lin, Jinny Claire Lee, Steven Blake, Beverly Ellis, Lisa M. Eubanks, and Kim D. Janda*

Cite This: *JACS Au* 2021, 1, 31–40

Read Online

ACCESS | Metrics & More | Article Recommendations | Supporting Information

**ABSTRACT:** Synthetic cannabinoids (SCs) constitute a significant portion of psychoactive substances forming a major public health risk. Due to the wide variety of SCs, broadly neutralizing antibodies generated by active immunization present an intriguing pathway to combat cannabinoid use disorder. Here, we probed hapten design for antibody affinity and cross reactivity against two classes of SCs. Of the 10 haptens screened, 3 vaccine groups revealed submicromolar $IC_{50}$, each targeting 5−6 compounds in our panel of 22 drugs. Moreover, SCs were successfully sequestered when administered by vaping or intraperitoneal injection, which was confirmed within animal models by observing locomotion, body temperature, and pharmacokinetics. We also discovered synergistic effects to simultaneously blunt two drug classes through an admixture vaccine approach. Collectively, our study provides a comprehensive foundation for the development of vaccines against SCs.

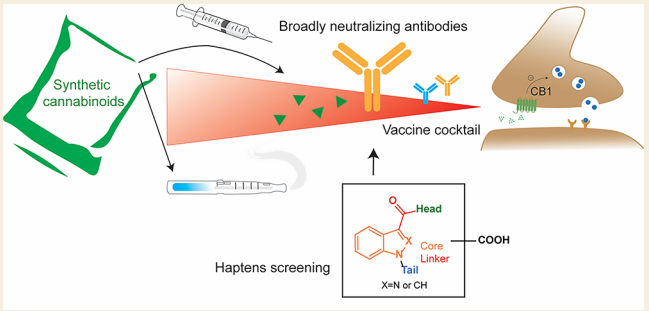


**KEYWORDS:** *synthetic cannabinoids, psychoactive substances, cannabinoid use disorder, antibodies, immunization, haptens, vaping*

## INTRODUCTION

Synthetic cannabinoids (SCs) constitute the largest, most diverse, and fastest growing group of new psychoactive substances (NPS) on the market.[1] They are referred to as synthetic substances acting on the endocannabinoid system, where CB1 receptors are predominantly responsible for their psychotropic effect. Designed to target the cannabis market with an expansive network of users worldwide, SCs are soaked in or sprayed onto plant materials and sold under a variety of names like "spice" or "K2".[2] Their higher receptor affinity and potency compared to THC, severity of health risks causing hospitalizations and fatalities, and variability in the quantity and number of active ingredients used in the product can be perilous to public health, especially in young adults in terms of prevalence and brain susceptibility.[3,4] To illustrate, there are 3.3% of high school seniors that reported SC use in the past year, according to statistics from The National Institute of Health on drug abuse, which is much higher than drugs like cocaine (2.2%), heroin (0.4%), and methamphetamine (0.5%). Their consumption steadily gives rise to thousands of emergency calls recorded by The American Association of Poison Control Centers each year and more than 10× the number of cases reported to The National Forensic Laboratory Information System.[5,6] The past decade has witnessed the intense interplay between SCs' increase in popularity as a form of "legal high" and generic national legislation to counteract its structural diversity. In response to these legislative practices, clandestine manufactory processes have produced over 250 substances to elude the standard drug test.[7]

This expansive production of substances was achieved by dividing the structure of SCs into four regions: core, linker, head, and tail (Figure 1). The most popular SCs are continuously composed of (1) an indole or indazole core; (2) a flanking carbonyl, amide, or ester linker; (3) a relatively conserved tail group largely limited to pentyl, fluoropentyl, benzyl, and cyclohexyl methyl; and (4) a more variable head moiety typically consisting of derivatives of naphthyl and valine.[8,9] Unlike the opioid crisis, currently available therapeutics only consist of symptomatic treatment of SC use disorder or overdose reversal.[10] In addition, the interaction of common drug metabolism enzymes, such as cytochrome P450s, complicate the severity of symptoms at the standpoint of drug−drug interactions because SCs are generally consumed with other drugs of abuse and undergo extensive metabolism.[11,12]

After successfully applying immunopharmacotherapeutics to combat opioids, cocaine, nicotine, and methamphetamine,[13−21] the occurrence of NPS requires optimized vaccine strategies through hapten design and vaccine cocktails for broad neutralization while maintaining sufficient binding efficacy.[22−24] This broad neutralization is necessary because SCs are often ingested as a cocktail of drug species, unlike

Received: October 20, 2020
Published: December 15, 2020

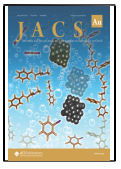

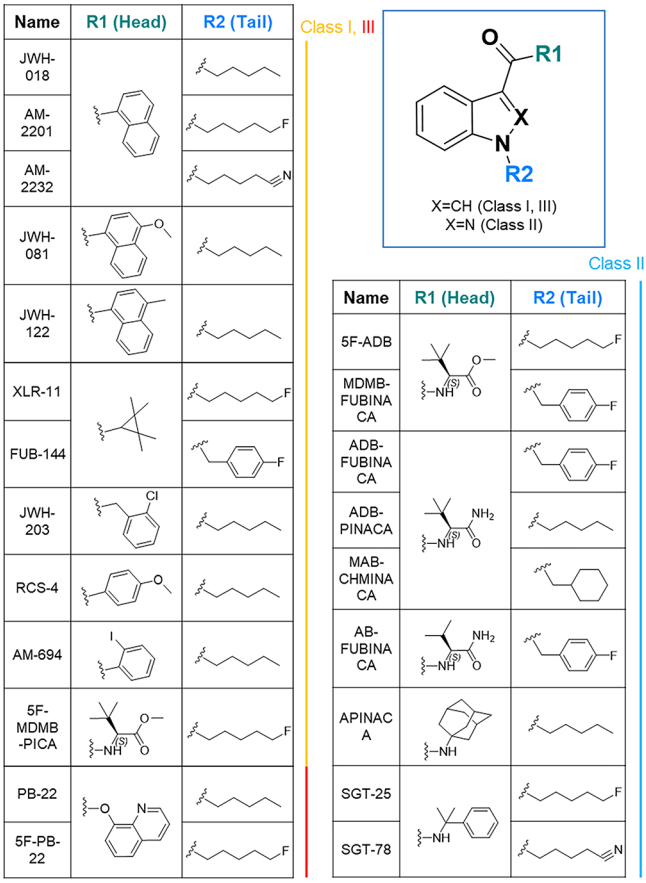


**Figure 1.** Structural framework of prevalent SCs and the selected drug catalogue in this study. Four fragments consisting of prevalent SCs, namely core, linker, head, and tail. Head and tail fragments are labeled as R1 and R2, respectively. The catalogue includes 22 selected drugs distributed in 3 classes with their structure composition listed.

cocaine and methamphetamine. Currently, intraperitoneal or intravenous drug administration are the gold standards to study behavior models in vaccinated animals. However, the rise in e-cigarette use,[25] in addition to traditional smoking methods, creates a necessity to investigate the effects of vaccines against vaporized drug models. This study initiates our effort to incorporate vaping into vaccine evaluation for SCs and contribute to the paradigm in vaccine efficiency studies for vaporized drugs.[26,27] Ten haptens were designed in a screening format to target SCs and their primary metabolites. *In vivo* efficacy of the best candidates and their combinations was tested in behavior models by administering the drug intraperitoneally or through a vaping apparatus.

## RESULTS AND DISCUSSION

Prior to hapten design, target drug molecules for vaccine formulation were selected based on their prevalence, severity, and diversity.[28] Twenty-two drugs implemented in the study were proportionally distributed among three classes: indole carbonyl (Class I), indazole amide (Class II), and indole ester (Class III) (Figure 1). The structural components of this catalogue covered: (1) the four common tail compositions: pentyl, fluoropentyl, benzyl, and cyclohexyl methyl; (2) all modifications of L-*tert*-leucine from amide to ester; and (3) the most potent naphthyl derivatives listed in the Drug Enforcement Administration (DEA) schedule I category. The catalogue also extended to other less-frequent fragments as substituents, such as adamantyl and tetramethylcyclopropyl. Within the first two main classes, derivatives of indole naphthyl and indazole valine constituted half of the drug catalogue; thus, these compounds became our primary vaccine targets. Rapid hapten synthesis was achieved by modifying previously reported synthetic methods on different subunits (see the synthesis section in the Supporting Information).[29]

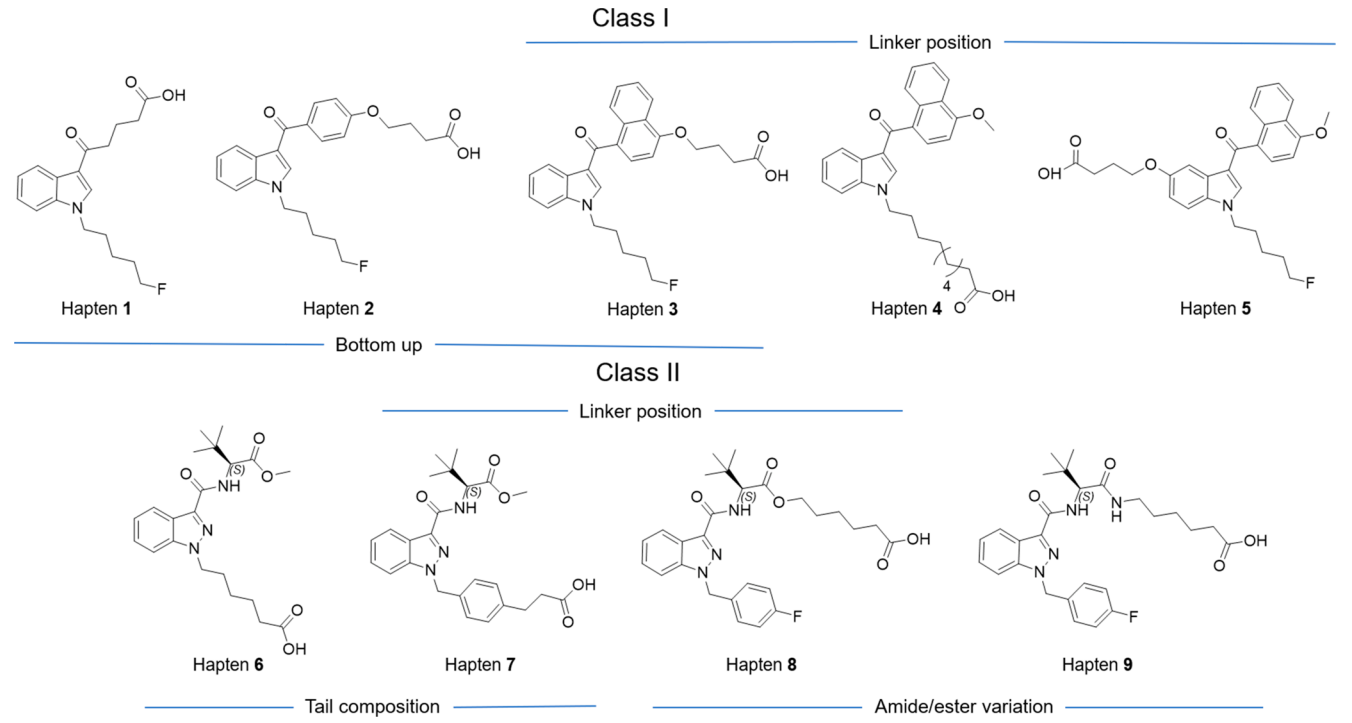


**Figure 2.** Hapten design. Two classes of haptens, five for Class I and four for Class II, categorized by the class of drugs they target.


https://dx.doi.org/10.1021/jacsau.0c00057
JACS Au 2021, 1, 31−40

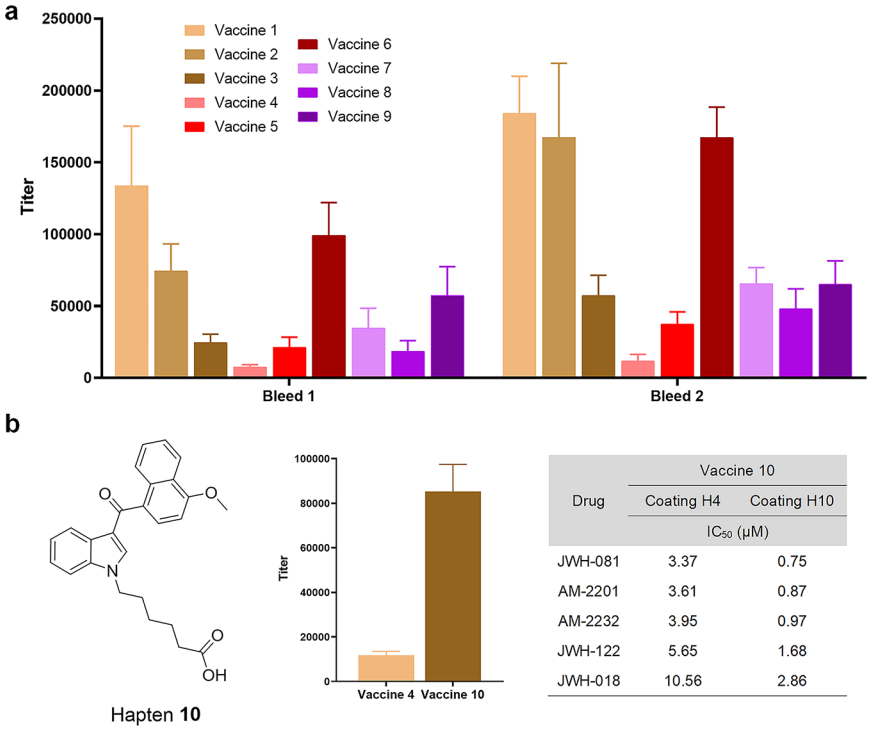


| Drug | Vaccine 10 | |
|---|---|---|
| | Coating H4 | Coating H10 |
| | $IC_{50}$ (μM) | |
| JWH-081 | 3.37 | 0.75 |
| AM-2201 | 3.61 | 0.87 |
| AM-2232 | 3.95 | 0.97 |
| JWH-122 | 5.65 | 1.68 |
| JWH-018 | 10.56 | 2.86 |

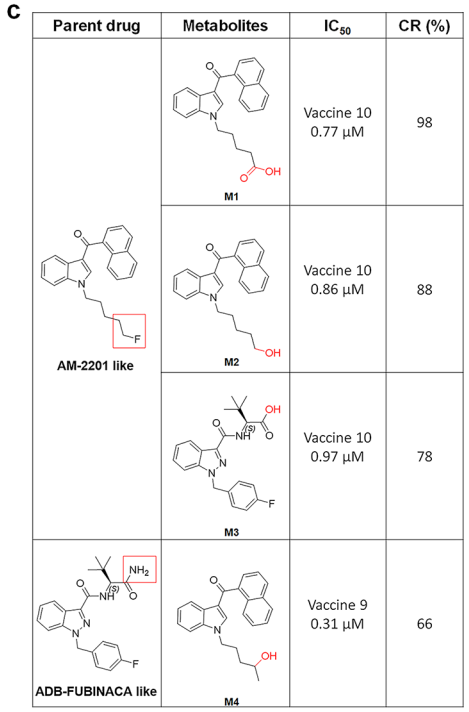


**Figure 3.** Immune response of screening vaccines. (a) Midpoint titers of vaccines **1**−**9**, using sera from vaccinated mice ($n$ = 6/group) on days 21 (bleed 1) and 35 (bleed 2). All bars are shown as mean ± SEM. (b) Structure of optimized hapten **10**. Titer comparison of vaccines **4** and **10** from second bleeding, and effects of two different coatings on drug $IC_{50}$ of vaccine **10** antisera. Assays are run using mice sera pooling from whole vaccine groups ($n$ = 6). (c) Metabolism patterns of two types of synthetic cannabinoids. Affinity are measured in vaccine **9** or **10** with cross reactivity calculated relative to JWH-081 or ADB-FUBINACA in Table 1.

**Table 1. Inhibition Concentration 50% ($IC_{50}$) and Cross Reactivity (CR) for Class I and Class II Vaccines against the Drug Panel**[a]

| | vaccine 1 | vaccine 2 | vaccine 3 | | vaccine 4 | | vaccine 5 |
|---|---|---|---|---|---|---|---|
| drug | $IC_{50}$ (μM) | $IC_{50}$ (μM) | $IC_{50}$ (μM) | CR (%) | $IC_{50}$ (μM) | CR (%) | $IC_{50}$ (μM) |
| JWH-081 | | | 3.86 | 100 | 1.94 | 100 | |
| AM-2201 | | | 5.03 | 77 | 2.04 | 95 | |
| AM-2232 | | | 6.85 | 56 | 2.16 | 90 | |
| JWH-122 | | | 7.81 | 49 | 3.37 | 58 | |
| JWH-018 | | | 14.25 | 27 | 6.37 | 30 | |
| RCS-4 | | 3.28 | 57.03 | 7 | | | |

| | vaccine 6 | vaccine 7 | vaccine 8 | | vaccine 9 | |
|---|---|---|---|---|---|---|
| drug | $IC_{50}$ (μM) | $IC_{50}$ (μM) | $IC_{50}$ (μM) | CR (%) | $IC_{50}$ (μM) | CR (%) |
| ADB-FUBINACA | | 35.03 | 0.31 | 96 | 0.21 | 100 |
| AB-FUBINACA | | 45.49 | 0.40 | 74 | 0.24 | 88 |
| MAB-CHMINACA | | | 1.68 | 18 | 0.28 | 74 |
| ADB-PINACA | | | 2.13 | 14 | 0.87 | 24 |
| MDMB-FUBINACA | | 0.21 | 0.29 | 100 | 2.12 | 10 |
| 5F-ADB | 0.67 | 13.81 | 1.68 | 18 | 6.33 | 3 |
| 5F-MDMB-PICA | 6.14 | | 6.34 | 5 | 36.98 | <1 |

[a]IC50 values are measured by competitive ELISA using mice sera pooling from each individual in every vaccine group ($n$ = 6). Compounds without over 50% inhibition in all vaccine groups are excluded from this table. CR values are calculated relative to the direct targeting drugs, the one with the highest affinity in the column. A blank cell means that no affinity was detected.

To systematically evaluate the upper limit of cross reactivity, a screening panel of haptens was designed for the two SC classes (Figure 2). We hypothesized the efficacy of utilizing a bottom-up strategy, where a specific subunit of the structure would be targeted, to generate more broadly neutralizing antibodies. The core and tail consists of a relatively conserved region in Class I and III, which increases the chance of specifically targeting these two drug classes. Therefore, the first series of haptens was designed with an alkyl (hapten 1), phenyl (hapten 2), or naphthyl (hapten 3) at the head region. Studies have demonstrated the critical effects of linker position in how the hapten is approached by immune cells.[30,31] Thus, in addition to investigating the generation of broadly neutralizing antibodies, haptens 3, 4, 5, 7, and 8 were modified at various


https://dx.doi.org/10.1021/jacsau.0c00057
JACS Au 2021, 1, 31−40

regions to understand the effect of linker placement on hapten immunogenicity. In this regard, Class I drugs can be modified at three sites: 4′ naphthyl, 5′ indole, and tail terminal. On the other hand, Class II can be modified at the *tert*-leucine/valine carboxyl and tail terminal. Comparative results for varying tail composition were fulfilled by haptens 6 and 7, while ester and amide variations on L-*tert*-leucine for haptens 8 and 9 allowed for observations in cross reactivity within two subtypes of Class II drugs. Collectively, five haptens were synthesized for Class I and four haptens for Class II. Through the rational application of orthogonal protection, we were able to retain the methyl ester on haptens while selectively deprotecting the other carboxylic acid for protein conjugation (see the hapten conjugation section in the Supporting Information). Following *N*-hydroxy-sulfosuccinimide (Sulfo-NHS) activation using carbodiimide resin, haptens were conjugated with KLH to obtain immunoconjugates with a controllable copy number around 20 (Tables S1 and S2, Figure S1). The immunoconjugates were formulated with alum and CpG ODN 1826 adjuvants to produce vaccines **1**−**9**, which were intraperitoneally delivered to male C57BL/6J mice according to an immunization schedule (Figure S2).

Antibody titers, affinity, and cross reactivity were assessed by enzyme-linked immunosorbent assay (ELISA) and competitive ELISA (see the ELISA part in the Supporting Information, Figures S14 and S19). More robust antibody titers were observed in vaccines with smaller hapten sizes, such as **1**, **2**, and **6** (Figure 3a). The $IC_{50}$ of antibodies against 22 drugs was screened within a competitive range, which was determined by checkboard assays (Table 1). Antibodies generated by vaccines **6** and **7** only interacted with their direct analogues, 5F-ADB and MDMB-FUBINACA, with submicromolar $IC_{50}$, which demonstrates the ability of these haptens to distinguish between the head and tail compositions of the target drug. Moreover, the replacement of an alkyl chain to a phenyl containing linker on the hapten of vaccine **7** caused a threefold affinity enhancement compared to vaccine **6**, which is an effect that has been observed in a previous study.[32] The most promising results came from vaccines **3**, **4**, **8**, and **9**, which showed the best affinities at a low micromolar range with the broadest cross reactivity against 5−6 drugs (>10%). Vaccines **3** and **4** cross-reacted against all naphthyl derivatives, while vaccines **1** and **2** failed to produce detectable $IC_{50}$, which indicated that the loss of the complete head fragment could not be compensated by the simplest aromatic system. Even with integration of a naphthyl fragment, the positioning of the linker at 5′ indole led to negligible affinity. Surprisingly, vaccines **8** and **9** presented dramatic differences in cross reactivity profiles. Antibodies raised against vaccine **9** produced higher affinities on various tail compositions, while vaccine **8** resulted in preference for amide variants. Such hapten design permitted vast drug-binding patterns with simple modifications. Further analysis of all vaccines against 5F-ADB, which contains an indazole core, and 5F-MDMB-PICA, consisting of an indole, confirmed altering the indazole to an indole core caused dramatically decreased antibody affinity. Class I vaccines exhibited poorer affinities, and because vaccine **4** exhibited the lowest titer response, it was optimized by shortening the linker chain by four carbons, resulting in hapten **10**. Shorter linkers have demonstrated abilities to increase antibody concentrations.[33] This optimized hapten exhibited a near eightfold titer enhancement with a slight decrease in affinity. Studies have shown fluctuations in ELISA sensitivity when coating with haptens of similar structures containing differences only in linker lengths.[34,35] Thus, we compared coating effects of haptens **4** and **10**. A fivefold decrease in $IC_{50}$ was observed, and we concluded that vaccine **10** exceeded **4** in affinity (Figure 3b, Figure S15, Table 1).

The submicromolar range $IC_{50}$ measured using hapten **4** as a coating antigen seems to convey more accurate affinity values for vaccine **10**. More sensitive spectroscopy methods, such as surface plasmon resonance, could not be used due to hydrophobicity issues posed by the drugs. In general, the $IC_{50}$ values measured by competitive ELISA tended to be inflated; thus, the corresponding $K_d$ values for antisera generated from vaccines **8**, **9**, and **10** were expected to be in the nanomolar range.[36] The antibody concentrations of these three vaccine groups were determined by interpolated titer ELISA (Figures S17).[37] Antibody concentrations ranged from 1.5−2.5 mg/mL and were comparably higher than those reported from methamphetamine and nicotine vaccines (Figure S18).[38,39]

Promising hapten candidates were implemented in further studies to observe their abilities to bind with primary metabolites. The main metabolites of drugs similar to AM-2201 and ADB-FUBINACA undergo pentyl or fluoropentyl hydroxylation, subsequent carboxylation, and primary amide/ester hydroxylation—all of which maintain activities toward CB1 receptors.[40,41] Thus, vaccine **10** from Class I and vaccine **9** from Class II were implemented in observing their abilities to produce antibodies capable of binding to primary metabolites. 4-Hydroxypentyl metabolites were synthesized from pentanone reduction and 5-hydroxypentyl metabolites from benzyl ether or acetyl ester deprotection (see the synthesis section in the Supporting Information). All three indole-based metabolites (M1−M3) and the indazole-based metabolite (M4) demonstrated affinities similar to their parent drugs (Figure 3c), which indicated antibody efficacy in binding to both parent drugs and primary metabolites.

Another challenge facing the field of SC abuse is the lack of screening tests available to confirm SC ingestion.[40] We improved the detection limit of SCs and their primary metabolites through antibody-based assays by using a heterogeneous coating strategy (Figure S20).[42] Pairings between antisera and coating antigens were selected by coupling haptens that maintained similar overall structures with slight variations in substituents. Of the 7 potential pairings, coating with hapten **2** and using antisera from vaccine **10** produced the most promising results, with near 30-fold sensitivity enhancement for all recognized drugs and metabolites (Table S5).

The efficacy of the vaccines was further assessed in mouse models. One drug from each class, AM-2201 for Class I and ADB-FUBINACA for Class II, were first selected as drug surrogates due to their high affinity, structural representativeness, and relevance to some severe clinical cases.[43,44] After evaluating the cannabinoids using various behavior models, such as the tetrad test and conditioned place preference (Table S3, Figures S3−S7), hypolocomotion and hypothermia were determined to be the best fit for assessing drug challenges. Vaccinated mice were challenged with either AM-2201 at 0.4 and 0.8 mg/kg or ADB-FUBIANCA at 0.5 and 1.0 mg/kg concentrations. The control group exhibited dose-dependent responses, where at higher doses, the drugs completely paralyzed the mice and caused a body temperature drop of 8 °C. We also defined epileptiform behaviors like intermittent


https://dx.doi.org/10.1021/jacsau.0c00057
JACS Au 2021, 1, 31−40

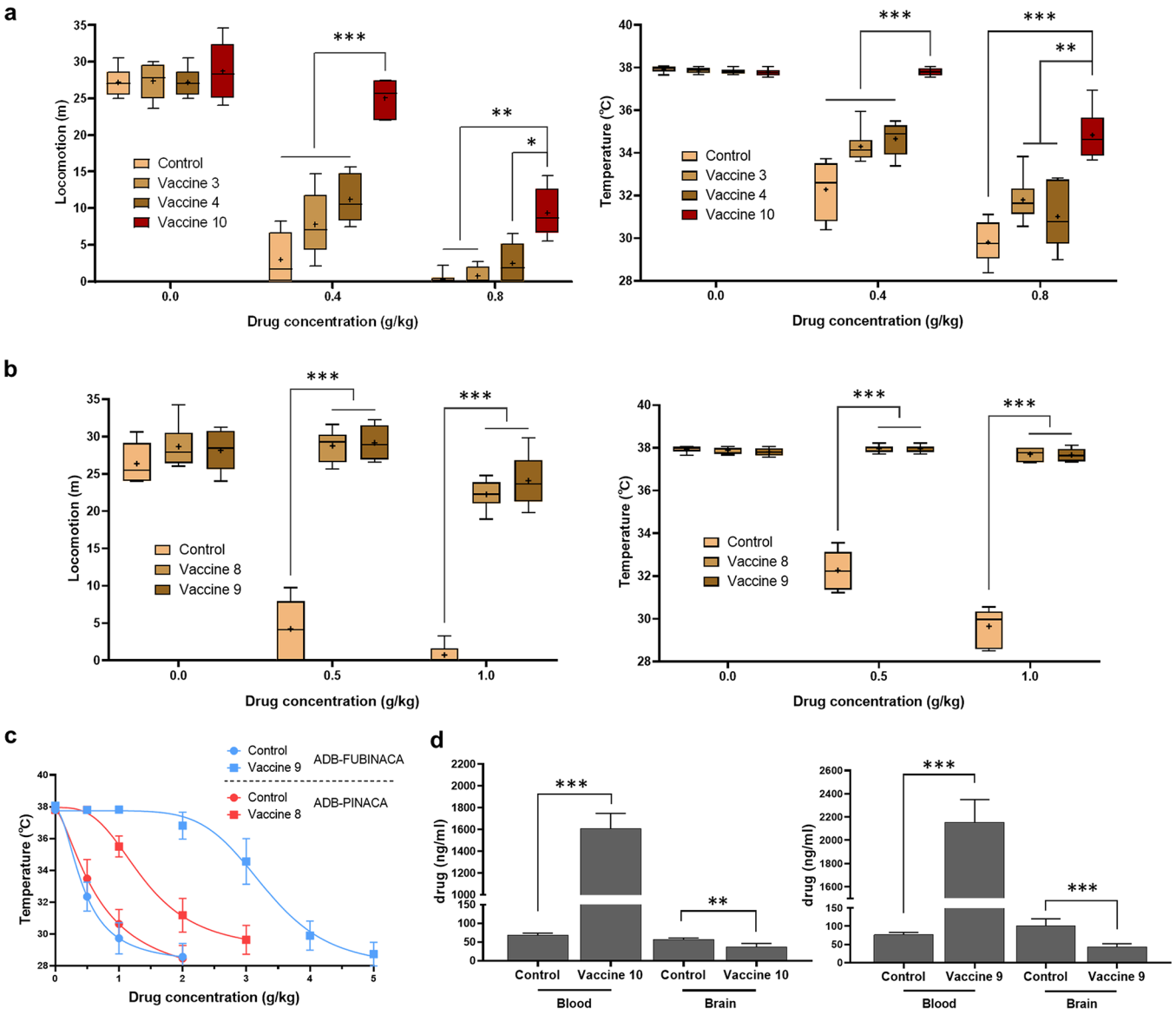


**Figure 4.** Vaccine efficacy by intraperitoneal drug administration. Behavior results in mice locomotion and body temperature of vaccines **3**, **4**, and **10** (a) and vaccines **8** and **9** (b), compared to the KLH vaccinated control mice. Mice accepted i.p. injection of each drug twice with different doses at 1 week intervals. Data are shown as median with quartiles ±10−90% CI ($n$ = 6); +, mean. Significance is denoted by asterisks determined by repeated-measures two-way ANOVA, Tukey multiple comparison test (***$P$ < 0.001, **$P$ < 0.01, *$P$ < 0.05). (c) Cumulative dose curve of drug effects on temperature. Mice of vaccines **8** and **9** were given ADB-PINACA and ADB-FUBINACA, respectively, and compared to KLH vaccinated control mice. Repeated administrations and temperature measurements were performed at 15 min intervals. Symbols are shown as mean ± SEM, ($n$ = 6). Nonlinear regression fit (inhibitor vs response, variable slope, 4 parameters, $IC_{50}$ = 0.44, 0.57, 1.40, 3.65 g/kg from low to high). (d) Blood-brain biodistribution of vaccines **10** and **9** vaccine groups using AM-2232 and ADB-FUBINACA as drug surrogates. All bars are shown as mean ± SEM ($n$ = 6). Significance is denoted by asterisks determined by unpaired $t$ test (***$P$ < 0.001, **$P$ < 0.01).

tonic-clonic jerking movements, jumping, and convulsion caused by both drugs.[45] Analysis of experimental vaccine cohorts demonstrated that vaccines **8**, **9**, and **10** conveyed full protection at low doses, while efficiencies at high doses varied (Figure 4a,b). Class II vaccines demonstrated better protective abilities, and vaccine **10** outperformed vaccines **3** and **4** in Class I, congruent with their higher affinities. All other vaccine groups presented low to no efficacy (Figures S8 and S9). To verify that the high cross reactivity could actually transform into broad protection, we tested the cumulative dose effect of ADB-PINACA in vaccine **8**, parallel with ADB-FUBINACA in vaccine **9**. Immunized mice showed a large ADB-FUBINACA $IC_{50}$ shift of nearly 7-fold and a 3-fold shift in ADB-PINACA with only 14% cross reactivity (Figure 4c).

From a pharmacokinetic standpoint, we investigated the effect of vaccines **9** and **10** on the biodistribution of a single SC dose. Drug concentration was quantified by liquid chromatography mass spectrometry using a standard addition method. Based on blank sera analysis spiked with drugs, we found AM-2232 had a relatively lower signal-to-noise ratio versus AM-2201, which was then served as a drug surrogate together with ADB-FUBINACA (Figure S10). Results indicated large increases of drug concentrations in the blood and decreased presence in the brain, which demonstrated the ability of the antibody to sequester over 20 times the amount of SCs,


https://dx.doi.org/10.1021/jacsau.0c00057
JACS Au 2021, 1, 31−40

relative to control mice, in the periphery prior to interaction with the central nervous system (Figure 4d).

Previous studies have used admixture vaccines, where two haptens are formulated into a single vaccine, to address the increasing instances of contaminated drug supplies, such as heroin containing traces of fentanyl.[46] A broadly neutralizing vaccine for SC use disorder would be ideal because the drug is often consumed in an impure form. Therefore, two combinations of haptens were selected by matching hapten **9** with two structurally distinct haptens from Class I. Admixture 1 consisted of haptens **3** and **9**, while admixture 2 incorporated haptens **9** and **10**. These formulations were administered at 50 $\mu$g of each hapten with the same adjuvants and vaccination schedules implemented earlier in the study. Compared to controls, there were no differences in antibody titer levels and affinities against Class I drugs (Figure S16, Table S4). However, results exhibited enhanced affinities against ADB-PINACA, 5F-ADB, and 5F-MDMB-PICA due to the shared pentyl tail in haptens of vaccines **3** and **10**. Due to the similar shape of haptens **3** and **9**, where the linker is attached to the head region, this observed effect was further enhanced in admixture 1 (Figure 5a). To confirm their *in vivo* efficacy, admixture 1 was challenged with ADB-PINACA in a cumulative dose manner, while admixture 2 sustained a combination mix consisting of 1.0 mg/kg ADB-FUBINACA and 0.5 mg/kg AM-2201. The cumulative dose curve

a

| Drug | Admixture 1 | | Admixture 2 | |
|---|---|---|---|---|
| | $IC_{50}$ (μM) | CR (%) | $IC_{50}$ (μM) | CR (%) |
| ADB-FUBINACA | 0.24 | 100 | 0.28 | 100 |
| AB-FUBINACA | 0.25 | 94 | 0.34 | 83 |
| MAB-CHMINACA | 0.38 | 63 | 0.34 | 83 |
| ADB-PINACA | 0.41 | 58 | 1.05 | 27 |
| MDMB-FUBINACA | 0.86 | 22 | 2.75 | 10 |
| 5F-ADB | 1.19 | 20 | 7.09 | 4 |
| 5F-MDMB-PICA | 4.69 | 5 | 32.45 | <1 |

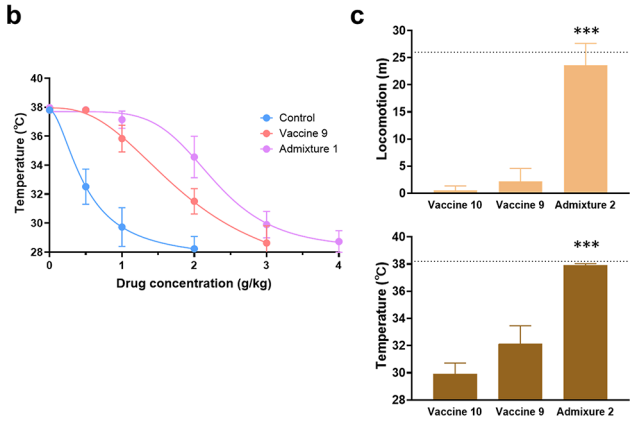


**Figure 5.** Immune response and vaccine efficacy of admixture vaccines. (a) $IC_{50}$ of admixture 1 and 2 vaccine groups against drugs in Class II. (b) Cumulative dose curve of the drug effect on temperature. Mice of nonvaccinated control, vaccine **9**, and admixture 1 were given ADB-PINACA. Same procedure as mentioned before. Symbols are shown as mean ± SEM, ($n$ = 6). Nonlinear regression fit (inhibitor vs response, variable slope, 4 parameters, $IC_{50}$ = 0.49, 1.80, 2.47 g/kg from low to high). (c) Behavior results of admixture 2 challenged with 1 mg/kg ADB-FUBINACA + 0.5 mg/kg AM-2201, in comparison to the individual vaccine groups. Dotted lines indicate the average of preinjected baseline ($n$ = 6). Significance is denoted by asterisks determined by one-way ANOVA and a Dunnett post hoc test (***$P$ < 0.001). All bars are shown as mean ± SEM.

experienced a right-shift, portraying enhanced affinity (Figure 5b). Admixture vaccine formulations permitted comprehensive protection against two drugs, which was not a capability observed through individual hapten vaccination (Figure 5c).

While most behavioral models challenge SCs vaccines through injection routes, we implemented a vaping administration route to mimic drug ingestion models most reflective of how SCs are used in reality (see vaping apparatus in Figure S11). Based on previously reported dose−effect relationships, we implemented 10 and 20 mg/mL (Figure 6a).[47] The

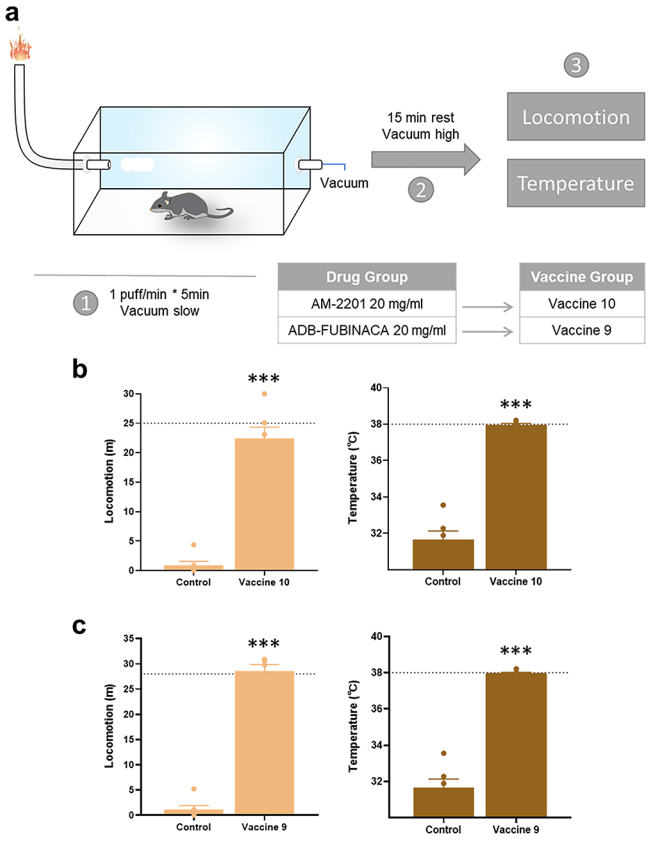


**Figure 6.** Vaccine efficacy by vaping drug administration. (a) Illustration of vaping apparatus and experimental schedule. Behavior results of Class I vaccine **10** (b) and Class II vaccine **9** (c) compared to the KLH vaccinated control group. Dotted lines indicate the average of preinjected baseline ($n$ = 6). Significance is denoted by asterisks determined by unpaired $t$ test (***$P$ < 0.001). All bars are shown as mean ± SEM.

apparatus parameters were set at 5 s/puff with 1 puff/min, an extreme condition that submerged mice in vapor conditions for 5 min. Faster onset and shortened duration of drug effects were observed in control mice (Figures S12 and S13). Thermolabile compounds, such as PB-22, were not good candidates in vaping settings, as they failed to produce desired drug effects (Figure S12). To closely compare the effects of drug administration routes on vaccine efficacy, 20 mg/mL of vaporized drug was applied because this concentration instigated similar drug responses as injection routes. An important phenomenon we observed during the vaping process was that drug inhalation caused faster drug effect onset in mice, but recovery occurred when administration ceased. This demonstrated the pharmacokinetic antagonism prompted by the antibodies generated through active vaccination. Both


https://dx.doi.org/10.1021/jacsau.0c00057
JACS Au 2021, 1, 31−40

vaccines **9** and **10** exhibited significant protective capabilities, evident through locomotion and body temperature recovery during drug challenges (Figure 6b, c).

## CONCLUSION

Herein, we devised a hapten screening system based on structure composition and linker position, permitting the discovery of three hapten candidates possessing submicromolar range $IC_{50}$ with the broadest cross reactivity for two drug classes of SCs. Drugs with a large number of derivatives at the head region containing either naphthyl or valine substituents enables the potential for numerous modifications at both the tail and head region for linker attachment; therefore, antibodies generated against these vaccines have a higher probability of achieving broad cross reactivity. In contrast, drugs with adamantyl and tetramethylcyclopropyl substituents permit the ability to insert linkers at the tail position. This causes issues with broad cross reactivity because tail linkers containing an alkyl chain or aromatic system can only interact with drugs containing similar substitutents.

We also found an admixture vaccine incorporating two haptens that could broaden the vaccine's targeting spectrum. The broadly neutralizing haptens and vaccine cocktail strategy expanded the drug recognition level of antibodies to more than 10 SC drugs. Although haptens with naphthyl derivatives produced weaker antibody affinities than valine derivatives, the difference in immunogenicity can be amended by implementing better carrier proteins, like tetanus toxoid, or adjuvants, such as derivatives from the polyphosphazene family.[48]

After confirming vaccine efficacy in behavior models by injection routes, we incorporated a vaping apparatus and successfully demonstrated that a small molecule vaccine had the potential to permit protective measures in a drug inhalation scenario. The increasing popularity of e-cigarettes raises concerns that drugs of abuse by vaping may become a serious public health concern, especially with the potential incorporation of more potent drugs like fentanyl and methamphetamine.[49] The direct comparison between vaccine efficacy in two administration models could serve as a paradigm for immunopharmacotherapeutics to combat any drugs of abuse that have ingestion routes of smoking or vaping.

SCs will continue to be central in leveraging cannabinoid receptors for euphorigenic effects, pain relief, and other recreational and therapeutic benefits.[50,51] While THC and many SCs are included within the federal government's schedule I list, new generations of SCs will never cease to enter the drug market. This work provides a basis in both chemistry design and biological models that provide tools to address the expanding cannabinoid crisis.

## METHODS

### Chemistry

Starting materials, reagents, and solvents were purchased from commercial vendors (Sigma-Aldrich, Combi-Blocks, etc.). All reactions were monitored by HPLC-MS and thin-layer chromatography (TLC) on Merck (0.25 mm thick, $60F_{254}$). Flash chromatography purification was performed on RediSep Rf Normal-phase Silica Flash Columns (60 Å pore size, 35−70 $\mu$m particle size, 230 to 400 mesh) using a gradient of hexane and EtOAc (with or without 0.05% acetic acid) as the mobile phase, and reversed-phase chromatography purification was performed on a RediSep Rf Gold Reversed-phase C18 column using a gradient of $H_2O$ (0.1% formic acid) and $CH_3CN$ (0.1% formic acid) as the mobile phase, both under the control of a Teltdyne ISCO Combiflash Rf+ Lumen column chromatography system. $^1H$ and $^{13}C$ NMR spectra were obtained on Bruker 600, 500, or 400 MHz spectrometers. Chemical shifts were given on the $\delta$ scale relative to internal $CDCl_3$ ($\delta$ 7.26, $^1H$ NMR; $\delta$ 77.16, $^{13}C$ NMR), DMSO-$d_6$ ($\delta$ 2.50, $^1H$ NMR; $\delta$ 39.52, $^{13}C$ NMR). Analytical LCMS was performed on an Agilent ESI-ToF (LC/MSD ToF) with an Agilent Zorbax 300SB-C8 (4.6 × 50 mm), 5 $\mu$m column using a flow rate of 0.5 mL/min. The LC-MS was run using the following solvents: Solvent A: 0.1% formic acid in $H_2O$, Solvent B: 0.1% formic acid in acetonitrile (MeCN), and each run was 10 min (0−7 min: 5−95% Solvent B, 7−10 min: 95% Solvent B). High resolution mass spectra (HRMS) were obtained at the Scripps Centre of Mass Spectrometry. HPLC spectra were recorded on an Agilent Systems 1260 using a Poroshell 120 EC-C8 column. The mobile phase gradient started from 95% $H_2O$ in acetonitrile to 95% acetonitrile over 5 min and then isocratic at 95% acetonitrile for 3 min at a 0.5 mL/min flow rate. Synthetic procedures for all drugs, metabolites, and haptens can be seen in Supporting Information.

### Animals

Eight-week old male C57BL/6J mice ($n$ = 6/group) were obtained from Jackson Laboratories. Each vaccinated group contained six mice and were group-housed in an AAALAC-accredited vivarium containing temperature- and humidity-controlled rooms, with mice kept on a reverse light cycle (lights on: 9 PM − 9 AM). All experiments were performed during the dark phase, generally between 1 PM − 4 PM. General health was monitored by both the scientists and veterinary staff of The Scripps Research Institute, and all studies were performed in compliance with the Scripps Institutional Animal Care and Use Committee (Protocol #08-0127-5) and the National Institutes of Health Guide for the Care and Use of Laboratory Animals.

### Vaccine Preparation

Haptens (2 mg) were activated by *N*-cyclohexylcarbodiimide, *N*′-methyl polystyrene (100 mg), and sulfo-NHS (8 mg) in DMF overnight, and use of LC-MS confirmed that over 85% yield was obtained. DMF was allowed to air-dry and dissolved in 400 $\mu$L of DMSO as a stock solution, which can be stored at −20 °C for a long period. For all haptens, conjugate efficiency was overwhelming using the traditional hapten to protein ratio. As a result, the optimal hapten ratio was evaluated by decreasing the initial concentration, and a nearly linear relationship was observed at the lower range (Figure S1). We concluded the 30 $\mu$L hapten stock on the 0.5 mg protein carrier is a good alternative for providing a suitable copy number. Solution of KLH conjugates was concentrated by Amicon Ultra Centrifugal Filters 10K MWCO at 5000 rpm until protein concentration was >0.5 mg/mL, which was verified by BCA assays and stored at 4 °C until formulation. Copy number for all haptens are listed (Table S2), and their MALDI graph is located in the Supporting Information. Copy number = (MALDI MS-66430)/(Hapten MW-18). For every 6 mice, 300 $\mu$g of hapten conjugates were then formulated with 3 g of Alum and 300 $\mu$g of CpG the day before immunization.

### ELISA (Titer)

Microtiter plates (Costar 3690) were incubated with coating antigen, hapten-BSA, 5 $\mu$g/mL, 25 $\mu$L/well at 4 °C overnight. The plates were then blocked by 5% nonfat milk in PBS, 50 $\mu$L/well, at room temperature for 45 min to get rid of nonspecific binding. The blocking buffer was dumped out. Mouse sera were diluted 1:100 in 1% BSA PBS solution. When titering, 25 $\mu$L of mouse serum was serially diluted 1:1 in 1% BSA PBS buffer (pH 7.4) across 12 columns starting at 1:200. The plates were incubated in a moist chamber at 37 °C for 2 h followed by washing 10 times using a shower head with $dH_2O$ before adding secondary antibodies. Peroxidase-conjugated donkey antimouse IgG (Jackson ImmunoResearch Laboratories, Inc.; Catalog # 715-035-151) was diluted 1:10 000 for ELISA according to the instructions. Secondary antibodies were added at 25 $\mu$L/well, and the plates were incubated in a moist chamber at 37 °C for 1 h. The plates were further washed 10 times with $dH_2O$. Each well was treated with 50 $\mu$L of developing reagent, TMB substrate kit (Thermo Pierce),


https://dx.doi.org/10.1021/jacsau.0c00057
JACS Au 2021, 1, 31−40

waiting for blue color to develop over 10 min before being quenched by 50 $\mu$L of 2 M $H_2SO_4$. Absorbance was read on a microplate reader (SpectraMax M2e Molecular Devices) at 450 nm. In GraphPad PRISM 8, absorbance values were fit using the log (inhibitor) vs normalized response−variable slope equation to determine midpoint titer.

### Competitive ELISA

Indirect competitive ELISA protocol was used according to this setting. Hapten-BSA antigen was diluted in PBS and mouse sera in 1% BSA PBS solution to an optimal concentration pair in the linear range for competition determined previously by checkerboard titration. Following the same coating steps in the ELISA assay, the drug solution was prepared by serially diluting 60 $\mu$L of 400 $\mu$M drug solution (0.5% DMSO, 0.5% Cremophor EL in 1% BSA PBS) 1:2 across 12 columns. Forty microliters of diluted sera was then added to the drug plates, resulting in 200 $\mu$M to 1 nM competitive range. Twenty-five microliters of such antibody−drug mixture was transferred into the coating plates, which were further incubated for 1.5 h at 37 °C, followed by the same steps in the ELISA titer assay.

### Locomotion and Body Temperature

During the middle of the dark cycle, mice were placed in a testing room with a white light source and remained in their home cages for 10 min to acclimate. Mice were intraperitoneally injected with either vehicle (5% DMSO, 5% Cremphor EL in saline) or synthetic cannabinoids 25 min before being placed in a plastic cage (267 × 483 × 203 mm) with a clear ventilated acrylic top to be recorded and tracked by overhead cameras using ANY-Maze video tracking software (Stoelting Co., Wood Dale, IL). The habituation period lasted for 4 days when all mice receiving saline were placed into locomotion cages 25 min after injection for a 10 min recording. The moving distance fluctuated a lot at first but became steady at the end of the period. For the preliminary behavior test, the mice were randomly distributed into control and drug groups each containing eight mice. On the testing day, the procedure remained the same except the vehicle or drug was given to the mice. Immediately after locomotion, the RET-3 nonisolated rectal probe (Physitemp Instruments, LLC) was applied for temperature measurement with 0.1 °F accuracy. The probe was lubricated before insertion and was cleaned by ethanol afterward. For the drug duration test, locomotion was not suitable given the habituation effect that occurred following repeated exposures which lead to the natural decrease of locomotion in the cage. The temperature was recorded at 15, 30, 60, 90, and 120 min after drug administration.

### Vaping

The aerosol was generated using a modified e-cigarette device (La Jolla Alcohol Research, Inc.) delivered to mouse-sized chambers. Device parameters and management were adjusted and conducted by Maury Cole, leader of the LJARI who is also a facility member of the Mouse Behavioral Assessment Core at Scripps Research. Mice were in pairs placed into the chambers and subjected to 10/20 mg/mL (PEG 400) of individual synthetic cannabinoid exposure. The dose was chosen to get a response similar to that seen in the i.p. injection. Aerosol was generated for 5 s (65 $\mu$L) every 1 min in a 5 min inhalation period. Mice were then rested in the chamber for 15 min with vacuum turned up before the same behavior testing as described in the former section.

### Blood-Brain Distribution

One week after the behavior study, mice were injected with AM-2232 (0.5 mg/kg) or ADB-FUBINACA (0.5 mg/kg) intraperitoneally. 15 min after injection, mice were fully anesthetized by isoflurane and decapitated rapidly using a guillotine. Trunk blood was collected while the brain was surgically removed, weighed, and placed in an Eppendorf tube with zirconium oxide beads (0.5 mm diameter, Thomas Scientific). For the brain tissue, ice-cold PBS buffer was added at a volume of 100 $\mu$L/0.1 mg, homogenized using a Bullet Blender (Next Advance, NY), and stored at −80 °C before further analysis. Trunk blood was centrifuged at 12 000 rpm for 15 min to collect the serum and stored at −80 °C as well. The standard addition method was applied to obtain the standard curve using blank mouse serum that had been spiked with known concentrations of synthetic cannabinoids. Fifty microliter aliquot of the blank brain homogenate and serum was added to 25 $\mu$L (50 ng/mL in ACN) of drug analogue as internal standard and 25 $\mu$L of spiked drug (gradient 1 $\mu$g/mL, 0.5 $\mu$g/mL, 0.2 $\mu$g/mL, 0.1 $\mu$g/mL, 50 ng/mL in ACN). The mixture was vortexed for 1 min to equilibrate or homogenized again using zirconium oxide beads for brain tissue, extracted into 400 $\mu$L of EtOAc by vortexing, and centrifuged at 3000 rpm for 5 min. A 300 $\mu$L aliquot of the upper layer was transferred into a new tube and evaporated using GENEVAC. Finally, samples were reconstituted in MeOH and sent for LC-MS analysis. The standard curves were plotted in Figure S10. The same procedure was applied to the testing sample except that 50 $\mu$L experimental samples and 25 $\mu$L of blank ACN were added instead of blank samples and spiked drug solution. The ion ratio of drug vs internal standard was plotted into standard curves to get the real concentration.

## ■ ASSOCIATED CONTENT

### Supporting Information

The Supporting Information is available free of charge at https://pubs.acs.org/doi/10.1021/jacsau.0c00057.

Detailed experimental protocols and results for drug and hapten synthesis, behavior experiments, ELISA assays, and NMR spectra (PDF)

## ■ AUTHOR INFORMATION


### Corresponding Author

**Kim D. Janda** − *Department of Chemistry, Department of Immunology and Microbial Science, The Skaggs Institute for Chemical Biology, and The Worm Institute for Research and Medicine (WIRM), The Scripps Research Institute, La Jolla, California 92037, United States;* orcid.org/0000-0001-6759-4227; Phone: (858) 785- 2515; Email: kdjanda@scripps.edu; Fax: (858) 784-2595

### Authors

**Mingliang Lin** − *Department of Chemistry, Department of Immunology and Microbial Science, The Skaggs Institute for Chemical Biology, and The Worm Institute for Research and Medicine (WIRM), The Scripps Research Institute, La Jolla, California 92037, United States;* orcid.org/0000-0002-3325-4539

**Jinny Claire Lee** − *Department of Chemistry, Department of Immunology and Microbial Science, The Skaggs Institute for Chemical Biology, and The Worm Institute for Research and Medicine (WIRM), The Scripps Research Institute, La Jolla, California 92037, United States;* orcid.org/0000-0001-6869-6671

**Steven Blake** − *Department of Chemistry, Department of Immunology and Microbial Science, The Skaggs Institute for Chemical Biology, and The Worm Institute for Research and Medicine (WIRM), The Scripps Research Institute, La Jolla, California 92037, United States;* orcid.org/0000-0002-3357-0515

**Beverly Ellis** − *Department of Chemistry, Department of Immunology and Microbial Science, The Skaggs Institute for Chemical Biology, and The Worm Institute for Research and Medicine (WIRM), The Scripps Research Institute, La Jolla, California 92037, United States*

**Lisa M. Eubanks** − *Department of Chemistry, Department of Immunology and Microbial Science, The Skaggs Institute for*




https://dx.doi.org/10.1021/jacsau.0c00057
JACS Au 2021, 1, 31−40

*Chemical Biology, and The Worm Institute for Research and Medicine (WIRM), The Scripps Research Institute, La Jolla, California 92037, United States;* orcid.org/0000-0001-5288-6294

Complete contact information is available at: https://pubs.acs.org/10.1021/jacsau.0c00057

### Notes

The authors declare no competing financial interest.

## ■ ACKNOWLEDGMENTS

We thank Amanda Roberts and Maury D. Cole from the Mouse Behavioral Assessment Core Facility, Scripps Research, for technical support on animal experiments and vaping setup. This project was supported by the Skaggs Institute for Chemical Biology. All images were created by the authors of this manuscript.

## ■ REFERENCES

(1) *World Drug Report 2019*, Sales No. E.19.XI.8; United Nations publication, 2019.
(2) Evans-Brown, M.; Gallegos, A.; Christie, R. *Fentanils and synthetic cannabinoids: driving greater complexity into the drug situation. An update from the EU Early Warning System*; Publications Office of the European Union, 2018.
(3) Castaneto, M. S.; Gorelick, D. A.; Desrosiers, N. A.; Hartman, R. L.; Pirard, S.; Huestis, M. A. Synthetic cannabinoids: Epidemiology, pharmaco-dynamics, and clinical implications. *Drug Alcohol Depend.* **2014**, *144*, 12−41.
(4) Trecki, J.; Gerona, R. R.; Schwartz, M. D. Synthetic Cannabinoid-Related Illnesses and Deaths. *N. Engl. J. Med.* **2015**, *373* (2), 103−107.
(5) Gummin, D. D.; Mowry, J. B.; Spyker, D. A.; Brooks, D. E.; Beuhler, M. C.; Rivers, L. J.; Hashem, H. A.; Ryan, M. L. 2018 Annual Report of the American Association of Poison Control Centers' National Poison Data System (NPDS): 36th Annual Report. *Clin. Toxicol.* **2019**, *57* (12), 1220−1413.
(6) National Forensic Laboratory Information System: *NFLIS-Drug 2018 Annual Report*; U.S. Drug Enforcement Administration: Springfield, VA, 2019.
(7) *2017 Global Synthetic Drugs Assessment*; United Nations Office on Drugs and Crime: 2017.
(8) Adams, A. J.; Banister, S. D.; Irizarry, L.; Trecki, J.; Schwartz, M.; Gerona, R. Zombie″ Outbreak Caused by the Synthetic Cannabinoid AMB-FUBINACA in New York. *N. Engl. J. Med.* **2017**, *376* (3), 235−242.
(9) Worob, A.; Wenthur, C. DARK Classics in Chemical Neuroscience: Synthetic Cannabinoids (Spice/K2). *ACS Chem. Neurosci.* **2020**, *11*, 3881.
(10) Tait, R. J.; Caldicott, D.; Mountain, D.; Hill, S. L.; Lenton, S. A systematic review of adverse events arising from the use of synthetic cannabinoids and their associated treatment. *Clin. Toxicol.* **2016**, *54* (1), 1−13.
(11) Chimalakonda, K. C.; Seely, K. A.; Bratton, S. M.; Brents, L. K.; Moran, C. L.; Endres, G. W.; James, L. P.; Hollenberg, P. F.; Prather, P. L.; Radominska-Pandya, A.; Moran, J. H. Cytochrome P450-Mediated Oxidative Metabolism of Abused Synthetic Cannabinoids Found in K2/Spice: Identification of Novel Cannabinoid Receptor Ligands. *Drug Metab. Dispos.* **2012**, *40* (11), 2174−2184.
(12) Toennes, S. W.; Geraths, A.; Pogoda, W.; Paulke, A.; Wunder, C.; Theunissen, E. L.; Ramaekers, J. G. Pharmacokinetic properties of the synthetic cannabinoid JWH-018 and of its metabolites in serum after inhalation. *J. Pharm. Biomed. Anal.* **2017**, *140*, 215−222.
(13) Bremer, P. T.; Schlosburg, J. E.; Banks, M. L.; Steele, F. F.; Zhou, B.; Poklis, J. L.; Janda, K. D. Development of a Clinically Viable Heroin Vaccine. *J. Am. Chem. Soc.* **2017**, *139* (25), 8601−8611.
(14) Bremer, P. T.; Kimishima, A.; Schlosburg, J. E.; Zhou, B.; Collins, K. C.; Janda, K. D. Combatting Synthetic Designer Opioids: A Conjugate Vaccine Ablates Lethal Doses of Fentanyl Class Drugs. *Angew. Chem., Int. Ed.* **2016**, *55* (11), 3772−3775.
(15) Olson, M. E.; Sugane, T.; Zhou, B.; Janda, K. D. Consequence of Hapten Stereochemistry: An Efficacious Methamphetamine Vaccine. *J. Am. Chem. Soc.* **2019**, *141* (36), 14089−14092.
(16) Kimishima, A.; Olson, M. E.; Natori, Y.; Janda, K. D. Efficient Syntheses of Cocaine Vaccines and Their in Vivo Evaluation. *ACS Med. Chem. Lett.* **2018**, *9* (5), 411−416.
(17) Lockner, J. W.; Lively, J. M.; Collins, K. C.; Vendruscolo, J. C. M.; Azar, M. R.; Janda, K. D. A Conjugate Vaccine Using Enantiopure Hapten Imparts Superior Nicotine-Binding Capacity. *J. Med. Chem.* **2015**, *58* (2), 1005−1011.
(18) Hambuchen, M. D.; Carroll, F. I.; Ruedi-Bettschen, D.; Hendrickson, H. P.; Hennings, L. J.; Blough, B. E.; Brieaddy, L. E.; Pidaparthi, R. R.; Owens, S. M. Combining Active Immunization with Monoclonal Antibody Therapy To Facilitate Early Initiation of a Long-Acting Anti-Methamphetamine Antibody Response. *J. Med. Chem.* **2015**, *58* (11), 4665−4677.
(19) Raleigh, M. D.; Baruffaldi, F.; Peterson, S. J.; Le Naour, M.; Harmon, T. M.; Vigliaturo, J. R.; Pentel, P. R.; Pravetoni, M. A Fentanyl Vaccine Alters Fentanyl Distribution and Protects against Fentanyl-Induced Effects in Mice and Rats. *J. Pharmacol. Exp. Ther.* **2019**, *368* (2), 282−291.
(20) Kosten, T. R.; Domingo, C. B.; Shorter, D.; Orson, F.; Green, C.; Somoza, E.; Sekerka, R.; Levin, F. R.; Mariani, J. J.; Stitzer, M.; Tompkins, D. A.; Rotrosen, J.; Thakkar, V.; Smoak, B.; Kampman, K. Vaccine for cocaine dependence: A randomized double-blind placebo-controlled efficacy trial. *Drug Alcohol Depend.* **2014**, *140*, 42−47.
(21) Cornuz, J.; Zwahlen, S.; Jungi, W. F.; Osterwalder, J.; Klingler, K.; van Melle, G.; Bangala, Y.; Guessous, I.; Muller, P.; Willers, J.; Maurer, P.; Bachmann, M. F.; Cerny, T. A Vaccine against Nicotine for Smoking Cessation: A Randomized Controlled Trial. *PLoS One* **2008**, *3* (6), e2547.
(22) Smith, L. C.; Bremer, P. T.; Hwang, C. S.; Zhou, B.; Ellis, B.; Hixon, M. S.; Janda, K. D. Monoclonal Antibodies for Combating Synthetic Opioid Intoxication. *J. Am. Chem. Soc.* **2019**, *141* (26), 10489−10503.
(23) McClenahan, S. J.; Kormos, C. M.; Gunnell, M.; Hambuchen, M. D.; Lamb, P.; Carroll, F. I.; Lewin, A. H.; Peterson, E. C.; Owens, S. M. Design, synthesis and biological evaluation of a bi-specific vaccine against alpha-pyrrolidinovalerophenone (alpha-PVP) and 3,4-methylenedioxypyrovalerone (MDPV) in rats. *Vaccine* **2020**, *38* (2), 336−344.
(24) Sulima, A.; Jalah, R.; Antoline, J. F. G.; Torres, O. B.; Imler, G. H.; Deschamps, J. R.; Beck, Z.; Alving, C. R.; Jacobson, A. E.; Rice, K. C.; Matyas, G. R. A Stable Heroin Analogue That Can Serve as a Vaccine Hapten to Induce Antibodies That Block the Effects of Heroin and Its Metabolites in Rodents and That Cross-React Immunologically with Related Drugs of Abuse. *J. Med. Chem.* **2018**, *61* (1), 329−343.
(25) Krishnasamy, V. P.; Hallowell, B. D.; Ko, J. Y.; Board, A.; Hartnett, K. P.; Salvatore, P. P.; Danielson, M.; Kite-Powell, A.; Twentyman, E.; Kim, L.; Cyrus, A.; Wallace, M.; Melstrom, P.; Haag, B.; King, B. A.; Briss, P.; Jones, C. M.; Pollack, L. A.; Ellington, S.; Epidemiology, L. I. R. Update: Characteristics of a Nationwide Outbreak of E-cigarette, or Vaping, Product Use-Associated Lung Injury - United States, August 2019-January 2020. *Mmwr-Morbid Mortal W* **2020**, *69* (3), 90−94.
(26) Pravetoni, M.; Keyler, D. E.; Raleigh, M. D.; Harris, A. C.; LeSage, M. G.; Mattson, C. K.; Pettersson, S.; Pentel, P. R. Vaccination against nicotine alters the distribution of nicotine delivered via cigarette smoke inhalation to rats. *Biochem. Pharmacol.* **2011**, *81* (9), 1164−1170.
(27) Nguyen, J. D.; Bremer, P. T.; Hwang, C. S.; Vandewater, S. A.; Collins, K. C.; Creehan, K. M.; Janda, K. D.; Taffe, M. A. Effective active vaccination against methamphetamine in female rats. *Drug Alcohol Depend.* **2017**, *175*, 179−186.

(28) *2019 Drug Enforcement Administration National Drug Threat Asssessment*; U.S. Drug Enforcement Administration: WA, 2020.
(29) Banister, S. D.; Moir, M.; Stuart, J.; Kevin, R. C.; Wood, K. E.; Longworth, M.; Wilkinson, S. M.; Beinat, C.; Buchanan, A. S.; Glass, M.; Connor, M.; McGregor, I. S.; Kassiou, M. Pharmacology of Indole and Indazole Synthetic Cannabinoid Designer Drugs AB-FUBINACA, ADB-FUBINACA, AB-PINACA, ADB-PINACA, 5F-AB-PINACA, 5F-ADB-PINACA, ADBICA, and 5F-ADBICA. *ACS Chem. Neurosci.* **2015**, *6* (9), 1546−1559.
(30) Wang, L. T.; Jiang, W. M.; Shen, X.; Li, X. M.; Huang, X. A.; Xu, Z. L.; Sun, Y. M.; Chan, S. W.; Zeng, L. W.; Eremin, S. A.; Lei, H. T. Four Hapten Spacer Sites Modulating Class Specificity: Nondirectional Multianalyte Immunoassay for 31 beta-Agonists and Analogues. *Anal. Chem.* **2018**, *90* (4), 2716−2724.
(31) Langer, N.; Steinicke, F.; Lindigkeit, R.; Ernst, L.; Beuerle, T. Determination of cross-reactivity of poly- and monoclonal antibodies for synthetic cannabinoids by direct SPR and ELISA. *Forensic Sci. Int.* **2017**, *280*, 25−34.
(32) Luo, L.; Wei, X. Q.; Jia, B. Z.; Yang, J. Y.; Shen, Y. D.; Hammock, B.; Dong, J. X.; Wang, H.; Lei, H. T.; Xu, Z. L. Modulating Linker Composition of Haptens Resulted in Improved Immunoassay for Histamine. *Biomolecules* **2019**, *9*, 770.
(33) Gooyit, M.; Miranda, P. O.; Wenthur, C. J.; Ducime, A.; Janda, K. D. Influencing Antibody-Mediated Attenuation of Methamphetamine CNS Distribution through Vaccine Linker Design. *ACS Chem. Neurosci.* **2017**, *8* (3), 468−472.
(34) Franek, M.; Diblikova, I.; Cernoch, I.; Vass, M.; Hruska, K. Broad-specificity immunoassays for sulfonamide detection: Immunochemical strategy for generic antibodies and competitors. *Anal. Chem.* **2006**, *78* (5), 1559−1567.
(35) Bao, H. J.; Fang, S.; Liu, Z. J.; Shi, H. Y.; Ye, Y. H.; Wang, M. H. Development of an Enzyme-Linked Immunosorbent Assay for the Rapid Detection of Haloxyfop-P-Methyl. *J. Agric. Food Chem.* **2010**, *58* (14), 8167−8170.
(36) Torres, O. B.; Antoline, J. F. G.; Li, F. Y.; Jalah, R.; Jacobson, A. E.; Rice, K. C.; Alving, C. R.; Matyas, G. R. A simple nonradioactive method for the determination of the binding affinities of antibodies induced by hapten bioconjugates for drugs of abuse. *Anal. Bioanal. Chem.* **2016**, *408* (4), 1191−1204.
(37) Stevens, M. W.; Gunnell, M. G.; Tawney, R.; Owens, S. M. Optimization of a methamphetamine conjugate vaccine for antibody production in mice. *Int. Immunopharmacol.* **2016**, *35*, 137−141.
(38) Pravetoni, M.; Keyler, D. E.; Pidaparthi, R. R.; Carroll, F. I.; Runyon, S. P.; Murtaugh, M. P.; Earley, C. A.; Pentel, P. R. Structurally distinct nicotine immunogens elicit antibodies with non-overlapping specificities. *Biochem. Pharmacol.* **2012**, *83* (4), 543−550.
(39) Duryee, M. J.; Bevins, R. A.; Reichel, C. M.; Murray, J. E.; Dong, Y. X.; Thiele, G. M.; Sanderson, S. D. Immune responses to methamphetamine by active immunization with peptide-based, molecular adjuvant-containing vaccines. *Vaccine* **2009**, *27* (22), 2981−2988.
(40) Diao, X.; Huestis, M. A. Approaches, Challenges, and Advances in Metabolism of New Synthetic Cannabinoids and Identification of Optimal Urinary Marker Metabolites. *Clin. Pharmacol. Ther.* **2017**, *101* (2), 239−253.
(41) Gamage, T. F.; Farquhar, C. E.; McKinnie, R. J.; Kevin, R. C.; McGregor, L. S.; Trudell, M. L.; Wiley, J. L.; Thomas, B. F. Synthetic Cannabinoid Hydroxypentyl Metabolites Retain Efficacy at Human Cannabinoid Receptors. *J. Pharmacol. Exp. Ther.* **2019**, *368* (3), 414−422.
(42) Lei, H. T.; Shen, Y. D.; Song, L. J.; Yang, J. Y.; Chevallier, O. P.; Haughey, S. A.; Wang, H.; Sun, Y. M.; Elliott, C. T. Hapten synthesis and antibody production for the development of a melamine immunoassay. *Anal. Chim. Acta* **2010**, *665* (1), 84−90.
(43) Lam, R. P. K.; Tang, M. H. Y.; Leung, S. C.; Chong, Y. K.; Tsui, M. S. H.; Mak, T. W. L. Supraventricular tachycardia and acute confusion following ingestion of e-cigarette fluid containing AB-FUBINACA and ADB-FUBINACA: a case report with quantitative analysis of serum drug concentrations. *Clin. Toxicol.* **2017**, *55* (7), 662−667.
(44) Rojek, S.; Klys, M.; Maciow-Glab, M.; Kula, K. A new challenge in forensic toxicology exemplified by a case of murder under the influence of a synthetic cannabinoid - AM-2201. *Leg. Med.* **2017**, *27*, 25−31.
(45) Funada, M.; Takebayashi-Ohsawa, M. Synthetic cannabinoid AM2201 induces seizures: Involvement of cannabinoid CB1 receptors and glutamatergic transmission. *Toxicol. Appl. Pharmacol.* **2018**, *338*, 1−8.
(46) Hwang, C. S.; Smith, L. C.; Natori, Y.; Ellis, B.; Zhou, B.; Janda, K. D. Improved Admixture Vaccine of Fentanyl and Heroin Hapten Immunoconjugates: Antinociceptive Evaluation of Fentanyl-Contaminated Heroin. *ACS Omega* **2018**, *3* (9), 11537−11543.
(47) Lefever, T. W.; Marusich, J. A.; Thomas, B. F.; Barrus, D. G.; Peiper, N. C.; Kevin, R. C.; Wiley, J. L. Vaping Synthetic Cannabinoids: A Novel Preclinical Model of E-Cigarette Use in Mice. *Subst. Abuse: Res. Treat.* **2017**, *11*, 1−8.
(48) Mutwiri, G.; Benjamin, P.; Soita, H.; Townsend, H.; Yost, R.; Roberts, B.; Andrianov, A. K.; Babiuk, L. A. Poly[di(sodium carboxylatoethylphenoxy)phosphazene] (PCEP) is a potent enhancer of mixed Th1/Th2 immune responses in mice immunized with influenza virus antigens. *Vaccine* **2007**, *25* (7), 1204−1213.
(49) Moussawi, K.; Ortiz, M. M.; Gantz, S. C.; Tunstall, B. J.; Marchette, R. C. N.; Bonci, A.; Koob, G. F.; Vendruscolo, L. F. Fentanyl vapor self-administration model in mice to study opioid addiction. *Sci. Adv.* **2020**, *6* (32), No. eabc0413.
(50) Hua, T.; Li, X. T.; Wu, L. J.; Iliopoulos-Tsoutsouvas, C.; Wang, Y. X.; Wu, M.; Shen, L.; Johnston, C. A.; Nikas, S. P.; Song, F.; Song, X. Y.; Yuan, S. G.; Sun, Q. Q.; Wu, Y. R.; Jiang, S.; Grim, T. W.; Benchama, O.; Stahl, E. L.; Zvonok, N.; Zhao, S. W.; Bohn, L. M.; Makriyannis, A.; Liu, Z. J. Activation and Signaling Mechanism Revealed by Cannabinoid Receptor-G(i) Complex Structures. *Cell* **2020**, *180* (4), 655−665.
(51) Mucke, M.; Phillips, T.; Radbruch, L.; Petzke, F.; Hauser, W. Cannabis-based medicines for chronic neuropathic pain in adults. *Cochrane Db Syst. Rev.* **2018**, *3*, CD012182.


https://dx.doi.org/10.1021/jacsau.0c00057
*JACS Au* 2021, 1, 31−40